Potential for using High Temperature Membranes in the Sulphur Trioxide Decomposition Stage of a Thermochemical Cycle

Ian Atkin[1], Geof H. Priestman[1], Derek C. Sinclair[2] and Ray W. K. Allen[1]
[1]Department of Chemical and Process Engineering, University of Sheffield, Mappin Street, Sheffield, S1 3JD, United Kingdom
[2]Department of Engineering Materials, University of Sheffield, Mappin Street, Sheffield, S1 3JD, United Kingdom

Introduction

The sulphur-iodine (SI) and Hybrid Sulfur (HyS) cycles are promising processes for massive scale hydrogen production. These thermochemical cycles take water as a feedstock and produce only hydrogen and oxygen, with no additional waste streams. Both cycles employ the high temperature thermal decomposition of sulphuric acid.

The sulphuric acid thermal decomposition process has two reaction steps. The sulphuric acid is first decomposed to sulphur trioxide and water. Equilibrium composition calculations for this first step show that very high yields of SO_3 are achieved at 600°C and 1 bar from a pure H_2SO_4 feed. Sulphur trioxide then further decomposes to sulphur dioxide and oxygen. The equilibrium position for SO_3 decomposition is such that temperatures higher than 600°C are required for high yields. From a pure H_2SO_4 feed at 1 bar, the SO_2 yield is around 52% at 700°C and 87% at 900°C.

The use of a membrane separation in the SO_3 decomposition process that could enhance the yield of SO_2 at a given temperature is examined in this work. This would allow the operation of such a process with a lower peak temperature, enabling the use of more readily available heat sources. Alternatively, it could allow greater reactor throughput for a given heat duty.

Continuous removal of a proportion of the O_2 produced by SO_3 decomposition would cause the SO_3 decomposition equilibrium position to be shifted such that a greater proportion of the SO_3 would be decomposed than would be the case for a simple equilibrium process.

There are two types of membrane that could be suitable, dense and microporous. Dense oxygen transport membranes transport oxygen through their crystal lattice by ionic conduction. Microporous membranes, where the mean pore diameter is much smaller than the mean free path of the gas molecules, exhibit Knudsen regime flow, whereby the separation factors between components are equal to the ratio of the square roots of the molecular weights of each component.

Notional layouts used for process simulations

Process simulations were carried out using two notional layouts: a simple catalytic reactor, with a membrane separator downstream and retentate recycling; and use of a notional catalytic membrane reactor (CMR) in lieu of the simple catalytic reactor.

A downstream separation membrane would permit a stream of non-equilibrium composition to be removed from the process. A fraction of the retentate is then recycled to

the reactor feed, with the remaining retentate removed as the process product. This process is illustrated in Figure 1.
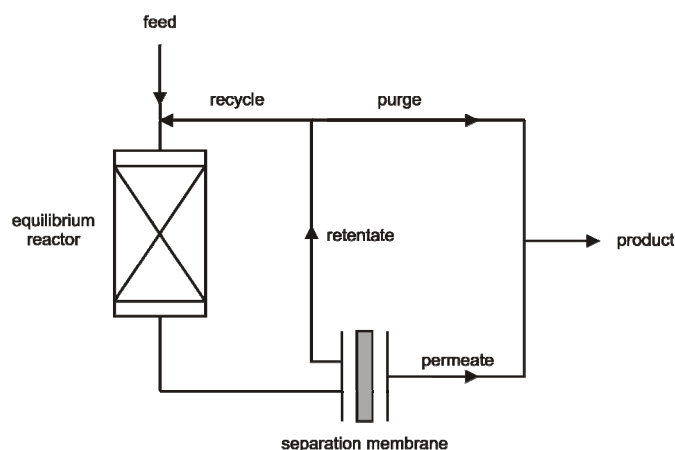

Figure 1: Schematic of downstream membrane separation/recycle process

The notional catalytic membrane reactor, as depicted in Figure 2, employs a number of tubular membranes inserted into a catalyst bed. The membranes selectively allow some products to permeate out of the catalyst bed, continuously shifting the reaction equilibrium and therefore potentially allowing a much greater yield of SO_2 than would be possible using a single equilibrium reactor.
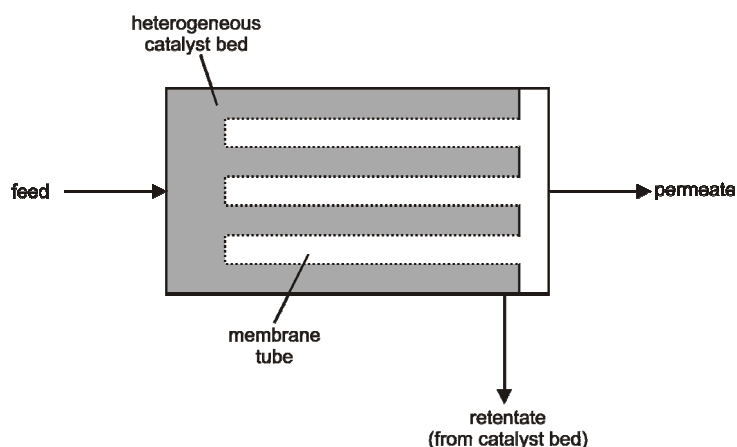

Figure 2: Schematic of catalytic membrane reactor (CMR) process

Forsberg [1] carried out a number of process simulations on the application of CMRs to the sulphuric acid thermal decomposition process. The simulations were made on the basis of a CMR with six theoretical 'stages', each allowing the process gas to come to equilibrium before performing a theoretically perfect separation. The simulations were replicated in order to validate the process simulation package used here, *ProSimPlus*.

Forsberg's work has been extended by carrying out a number of process simulations using both the CMR and downstream separation processes. Dense oxygen separation membranes and Knudsen regime porous membranes have been simulated with each process.

Specification for simulations

Each of the proposed process configurations have been modelled using the *ProSimPlus* steady state process simulation package. The components used for the simulations were H_2SO_4, H_2O, SO_2, SO_3 and O_2. A stream consisting of 92.7wt% H_2SO_4 and 7.3wt% H_2O entered the process and was subsequently heated to the required temperature. This acid concentration mirrors that specified by the original General Atomic flowsheet for the SI cycle acid decomposition section feed [2]. Simulations were carried out at 900K ≥ T ≤ 1300K in 100K steps and 1 atm (1.01325 bar(a)) ≥ P ≤ 30 bar(a). The reactors are modelled as gas phase equilibrium reactors performing a Gibbs free energy minimisation at the specified process temperature.

The dense oxygen separation membranes were simulated for the separation ratio, having values, F = 10, 100, 1000 and 10000. F is defined as:

$$F = \frac{\left(\frac{[O_2]}{[x]}\right)_{permeate}}{\left(\frac{[O_2]}{[x]}\right)_{feed}}$$

where x is each of the other species present. For dense membranes, these separation factors basically represent cross-membrane leakage, either as a result of membrane defects or poor sealing. The porous membranes were simulated as exhibiting Knudsen regime separation factors.

The overall yield of SO_2 was recorded for each simulation. For these simulations the SO_2 yield is equal to:

$$Y = \frac{\text{mols of } SO_2 \text{ in product}}{\text{mols of } H_2SO_4 \text{ in feed}}$$

Catalytic membrane reactor simulations

These simulations extended Forsberg's CMR simulation work by examining the SO_2 yield that could be achieved using CMRs of two to six theoretical equilibrium/separation stages. Additionally, separations with finite selectivity were employed. Figure 3 shows a typical *ProSimPlus* process layout for six theoretical 'stages'. It can be seen that the feed is heated then fed into a train of equilibrium reactors that are each followed by a separator, operating to a given selectivity. The products from each stage are mixed to produce the final product.
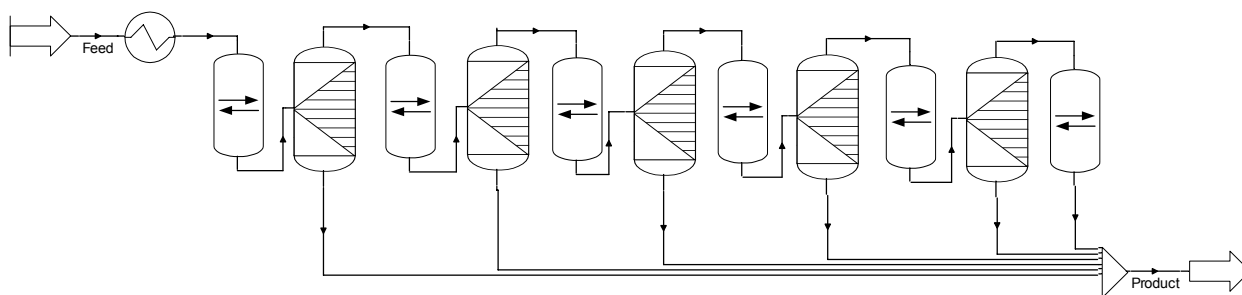
Figure 3: Typical *ProSimPlus* process layout for catalytic membrane reactor process simulations showing six theoretical equilibrium stages

As shown in Figure 4, increasing the number of theoretical stages beyond six produced little increase in SO_2 yield with the dense membrane simulations, whilst using more than two theoretical stages with microporous selectivity gave little improvement. This can be attributed to the flow rates through each stage. With the microporous membranes, the selectivity was sufficiently low that only a small proportion of the process flow was retained after the first two separation steps – most of the flow had "permeated" the membranes and passed out of the process. Because of this, the subsequent stages had very low flow rates and hence had little effect on the process as a whole. The selectivities relating to dense membranes were higher and hence a greater flow reached the later stages of the "train". Even here though, the flow rate was small once the eighth theoretical stage was reached.
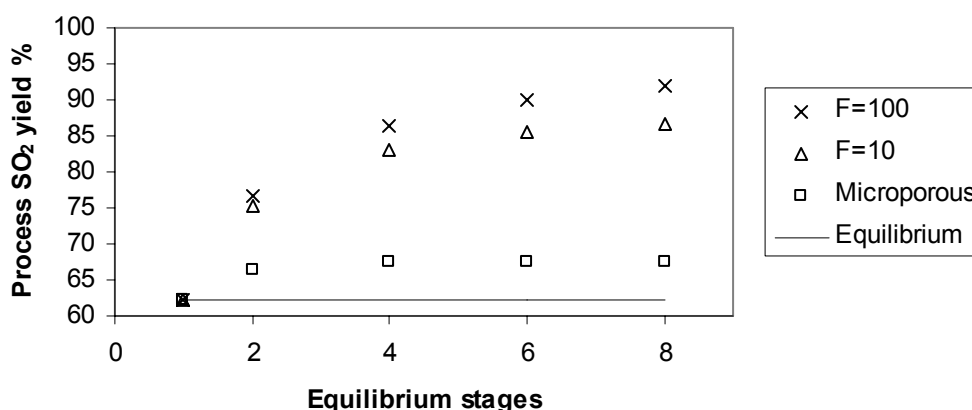

Figure 4: *ProSimPlus* CMR process simulations at 1 atm, 1000K and 92.7wt% H_2SO_4 feed

As the process temperature increases, the difference between the equilibrium SO_2 yield and the improved yields calculated by these simulations decreases (see Figure 5.) Because the equilibrium SO_2 yield increases with temperature, the scope for yield improvements decreases. The simulations suggest that at 1 atm and 1000K, using dense oxygen separation membranes and six theoretical stages, SO_2 yield could be increased from 62% to 85% or more. However, the same system at 1300K has an equilibrium yield of 95% and a dense membrane CMR yield of 99%, a higher absolute yield but a smaller improvement. It is because of this that it is thought that the CMR would be most beneficial to processes operating the sulphuric acid decomposition step at relatively low temperatures.
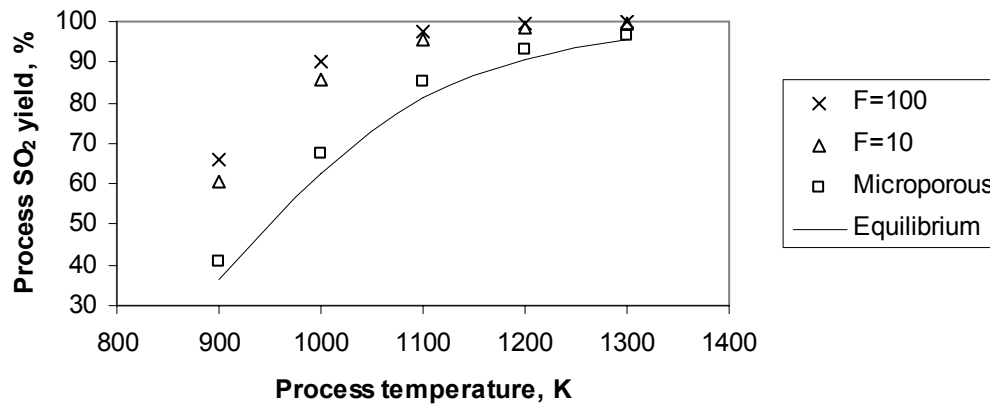
Figure 5: *ProSimPlus* CMR process simulations with six theoretical equilibrium/separation "stages", 1 atm and 92.7wt% H_2SO_4 feed

Downstream separation/recycle process simulations

The second part of the simulation work examined the potential for use of a downstream membrane separation and subsequent recycle, as opposed to the more complex CMR design.

The *ProSimPlus* simulations replicate the process depicted in Figure 1. The initial heated feed passes into the equilibrium reactor. A proportion of the reactor outlet stream passes through the membrane. A fraction of the membrane retentate is recycled and the remainder of the retentate is mixed with the membrane permeate to produce the process outlet stream. Recycle fractions of 20% ≥ R ≤ 80% in 20% steps were used. It was assumed that 75% of the oxygen entering the separation step permeated through the membrane.

It was calculated that SO_2 yield increases with increasing process temperature, increasing recycle ratio and increasing membrane separation factor. As with the CMR simulations, the SO_2 yield increase over the equilibrium value is greatest at lower temperatures where the equilibrium yield is relatively low. Figure 6 shows a typical set of results at 1000K and 1 atm, demonstrating that Knudsen regime microporous membranes give smaller yield increases than dense membranes under the same conditions.
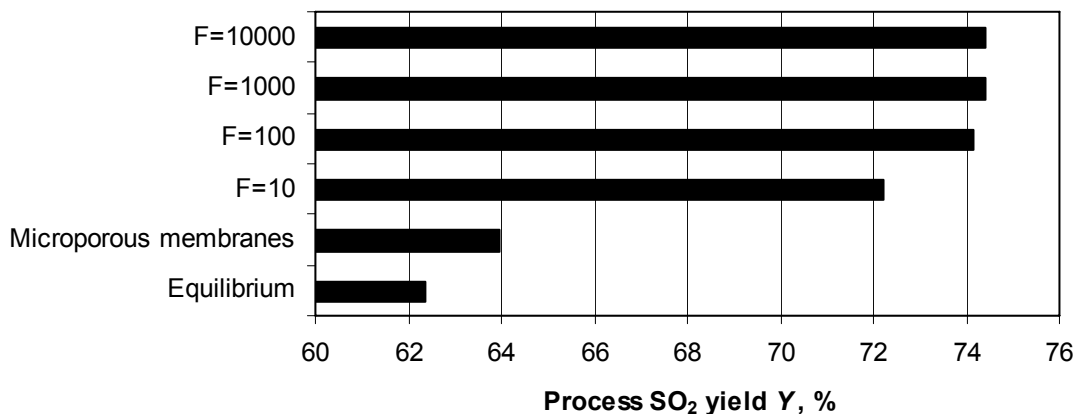

Figure 6: Downstream separation/recycle, 75% membrane O2 permeation, R=80%, T=1000K, feed of 92.7wt% H_2SO_4, P=1 atm

The data in Figure 6 also shows that increasing the selectivity of a dense membrane above 100 has a negligible effect on SO_2 yield. Since dense membranes are inherently gas tight, reduced selectivity might be caused by physical defects in the membrane or poor sealing.

Comparison of membrane separation processes

Comparing Figure 4 and Figure 6, which show simulation data at 1 atm and 1000K for CMR and downstream separation processes respectively, demonstrates that the CMR layout may produce greater SO_2 yield increases than the downstream separation, even for a CMR corresponding to two theoretical equilibrium/separation "stages". On this basis alone, the CMR seems the better of the two notional layouts. However, fabrication of a CMR may present greater challenges than a downstream separation, in terms of required membrane shape, sealing, etc. Therefore, if a modest increase in yield is acceptable, the simpler construction of a downstream membrane process may be sufficient.

Experimental work: YSZ as a potential membrane material

Experiments were carried out to assess the performance and longevity of yttria-stabilised zirconia (YSZ) when used for oxygen separation in the sulphuric acid decomposition section. YSZ powder (containing 8% yttria) was pressed and sintered to form pellets of approximately 24mm diameter and 2mm thickness. The pellets were then coated with either platinum or gold paste and heated to remove the paste's organic binder to leave a porous metallic electrode on each face. X-ray diffraction (XRD) and impedance spectroscopy (IS) data were recorded before the pellets were used. Comparing before and after XRD data (collected at ambient conditions) will indicate the presence of any additional phases in the pellet following the SO_2 exposure, whilst the IS data (collected at temperatures in the range 200-500°C) will show any changes in the conductivity of the bulk YSZ itself or of the grain boundaries within the sintered pellet. Any surface layer created on the pellet could also be identified from the IS data.

SO_2 exposure of 8% YSZ/Pt pellet at 900°C

A YSZ-Pt pellet was assembled into a bespoke quartz holder (Figure 7,) with external compression and gold foil gaskets sealing the assembly. The gold foil doubled as the electrical linkage of each pellet electrode to the external electrical circuitry, via the metalwork supporting the pellet holder. The apparatus was assembled inside a Carbolite tubular furnace. As shown in Figure 8, the outlet of the quartzware was connected on the permeate side to a Servomex gas analyser, measuring oxygen concentration, whilst the feed side vented to atmosphere.
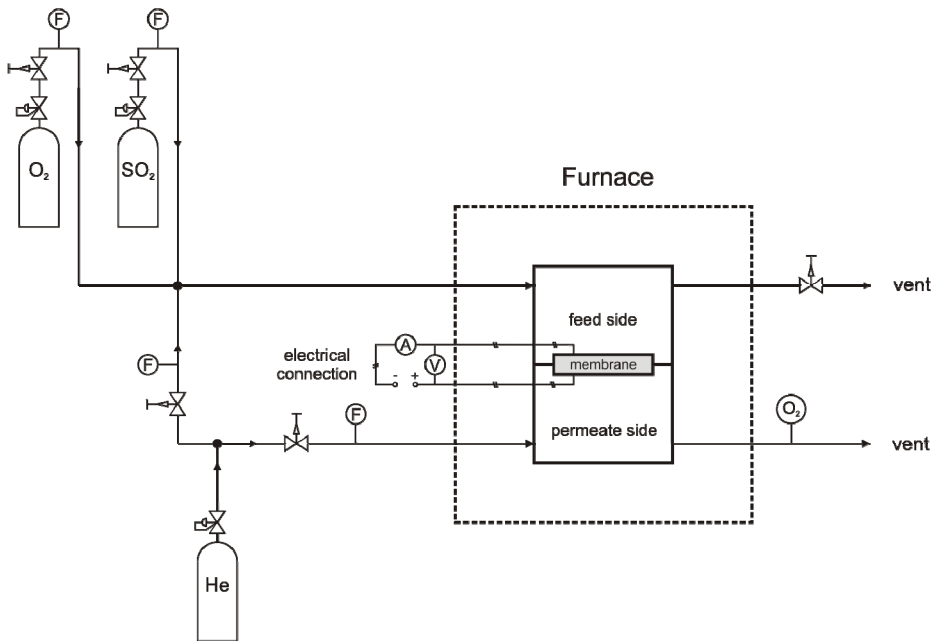
Figure 8: Schematic of experimental apparatus

Figure 7: Custom designed quartz membrane holder

The apparatus was heated to 900°C. The feed was 50ml/min of 30% SO_2 and 10% O_2 in He. The permeate side was supplied with 100ml/min of helium. A voltage of 1.00V was applied across the pellet. The current and permeate oxygen concentration were recorded. The feed side of the membrane was exposed to 50ml/min of 30% SO_2 and 10% O_2 in He for 870 minutes over three days. The experiment was ended after 870 minutes as the recorded values had reached a pseudo steady state and it was considered that further exposure time would be of little interest.
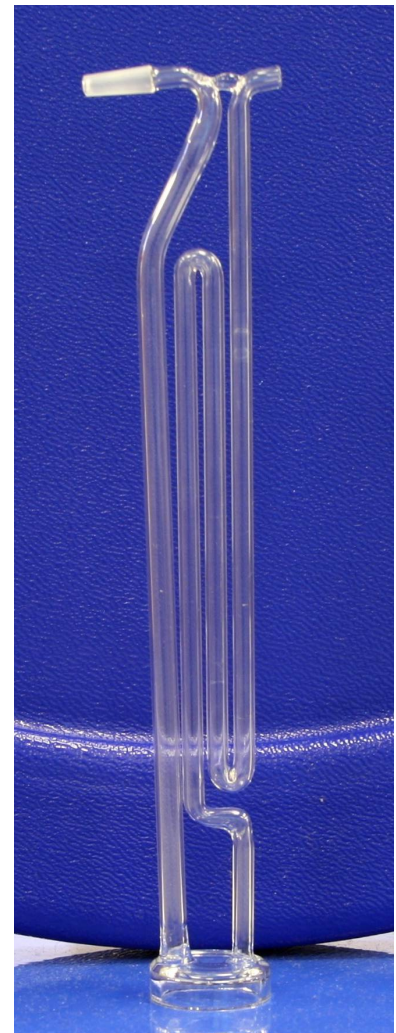
At the end of each day's SO_2 exposure period, the permeate oxygen concentration for zero applied voltage was recorded and this value was subtracted from the values recorded that day in order to produce a 'corrected' permeate oxygen concentration representing that oxygen which is being transported through the membrane as a result of the applied voltage and not because of internal electronic
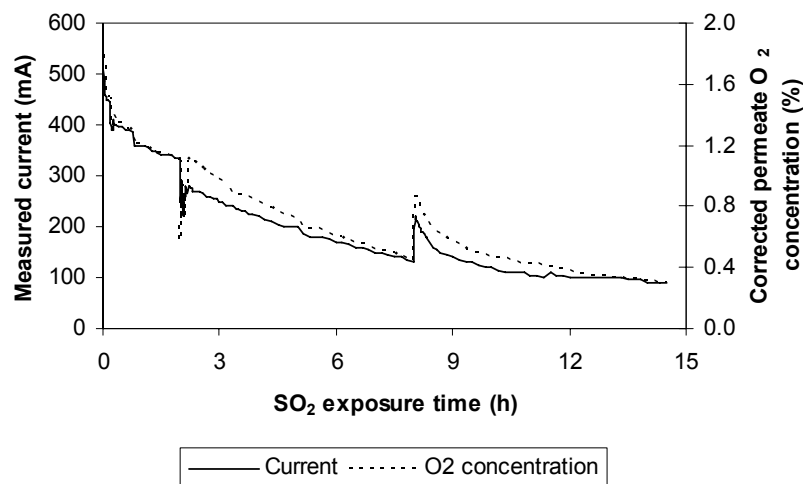

Figure 9: Measured current and corrected measured permeate oxygen concentration for 1.00V applied

transport. The resulting data is shown in Figure 9.

The abrupt changes at 2 and 8 hours signify the start and end points of each day's run. There were some electrical connection problems at the start of the second day, which manifest themselves as the low current values for around two hours. This may also explain the reason why the general trend for the second day is for lower currents compared to days one and three.

Fuming was observed from the feed side outlet during the run. Allowing dampened universal indicator paper to contact the fumes produced a strongly acidic response. Furthermore, a brown liquid collected at the lowest point in the straight quartz cooling tube downstream of the feed side of the membrane. When exposed to air during disassembly, this liquid fumed strongly. These two observations suggest that SO_3 is being produced in the feed side of the experimental apparatus. Given that the reaction rate for the SO_3 decomposition equilibrium reaction is very slow in the absence of catalyst, this indicates that the platinum electrode is catalytically active and is causing a proportion of the supplied SO_2 and O_2 to react and hence move towards the equilibrium position of the SO_3 decomposition step. Further work is in hand to determine the significance of this effect.

SO_2 exposure of 8% YSZ/Pt and 8% YSZ/Au pellets at 800°C

Having investigated the use of an 8% YSZ pellet with Pt electrodes at 900°C, a similar membrane was then tested at 800°C in order that the relative longevity could be measured. Previous equilibrium studies (Figure 10) indicated that zirconia should not suffer sulphation above 600°C. Because of this, a given YSZ membranes exposed to SO_2 at 800°C should not experience a greater percentage decrease in O_2 permeation performance than was recorded at 900°C. An identical YSZ pellet (pressed and sintered at the same time as the YSZ/Pt pellet) but with gold electrodes instead of platinum was tested to compare the O_2 permeation performance and to check if gold electrodes promoted the same catalytic activity seen with platinum electrodes which caused SO_3 to be produced from the SO_2/O_2 feed.
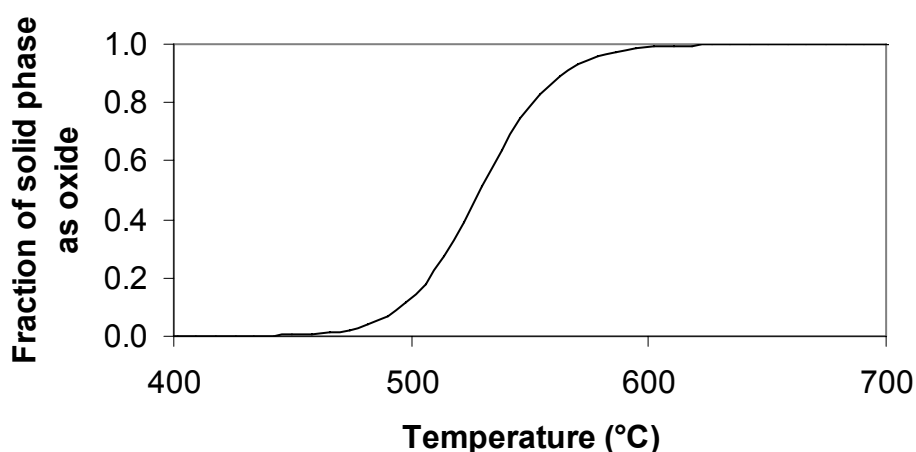

Figure 10: Equilibrium data from *HSC Chemistry* for a solid $ZrO_2/Zr(SO_4)_2$ phase in a gaseous $H_2SO_4/SO_3/SO_2/O_2/H_2O$ phase at 1 bar

The method employed was identical to that used for the 900°C run described previously, except that the ultimate furnace temperature was 800°C not 900°C. Once at 800°C, with 1.00V being applied across the electrode faces, the feed side was supplied with 10% O_2 in

He (total 50ml/min) for one hour. The feed was then changed to 30% SO_2 and 10% O_2 in He (total 50ml/min) for two hours. Between 60 and 90 minutes into this two hour SO_2 exposure period the electrical circuit was opened. This was carried out in order to determine if any increase in the O_2 permeate concentration occurred after a "rest" period of no externally applied voltage. Following the two hour SO_2 exposure period, the feed changed to 10% O_2 in He (total 50ml/min) for one hour. Finally, the feed reverted to 30% SO_2 and 10% O_2 in He (total 50ml/min) for one additional hour, before the experiment was ended.

The measured permeate O_2 concentrations are presented in Figure 11 for the YSZ/Pt membrane and Figure 12 for the YSZ/Au. Additionally, Table 1 shows some of the key comparison data between the platinum and gold electroded membranes.
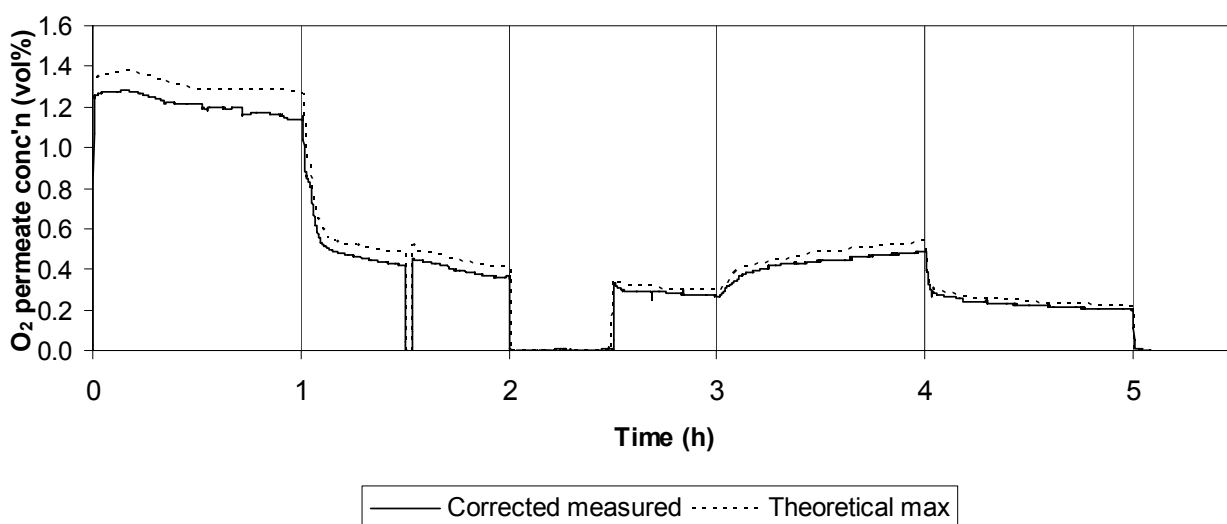

Figure 11: Data for exposure of 8% yttria YSZ pellet with platinum electrodes to SO_2 at 800°C – theoretical O_2 concentration is that calculated from the simultaneous current readings
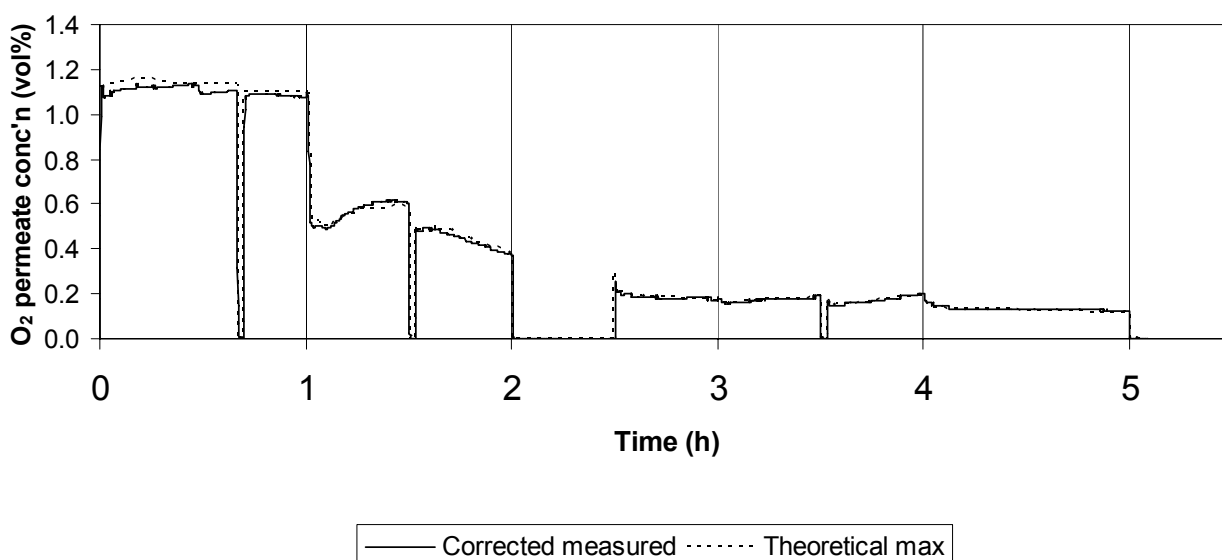

Figure 12: Data for exposure of 8% yttria YSZ pellet with gold electrodes to SO_2 at 800°C – theoretical O_2 concentration is that calculated from the simultaneous current readings

Table 1: Selected data from SO₂ exposure tests of 8% yttria YSZ pellets at 800°C

Permeate O$_2$ concentration (%) measurement time	Electrode	
	Pt	Au
Initial	1.25	1.13
After 1h O$_2$-He feed	1.14	1.07
After 10m SO$_2$-O$_2$-He feed	0.49	0.54
After 2h SO$_2$-O$_2$-He feed	0.26	0.17
After further 1h O$_2$-He feed	0.49	0.20
After final 1h SO$_2$-O$_2$-He feed	0.21	0.12

	Pt	Au
Ratio after:before further 1h O$_2$-He	1.88	1.18
Ratio initial:final	5.95	9.42

Table 1 shows the final O$_2$ concentration to be 1/5.95 of the initial value for the YSZ/Pt pellet at 800°C. This is very similar to the value recorded at 900°C (see Figure 9.) The fact that the fractional reduction in O$_2$ permeation flux is independent of temperature suggests the absence of a problem with pellet temperature such that the pellet is at a lower temperature than expected and is becoming affected by sulphation (see Figure 10.) Figure 13 shows the combined conductivity of the bulk YSZ in the pellet and the boundaries between the YSZ grains in the sintered mass. There is no significant change in the conductivity following the SO$_2$ exposure, which indicates that the "bulk" of the pellet is electrically unaffected. This leads to the conclusion that the reduction in permeate O$_2$ concentration and associated current flow is caused by a surface effect. Other IS and XRD data suggests that the loss of oxygen permeation performance is caused by the creation of a resistive surface layer. Investigations into the nature of this layer are ongoing.
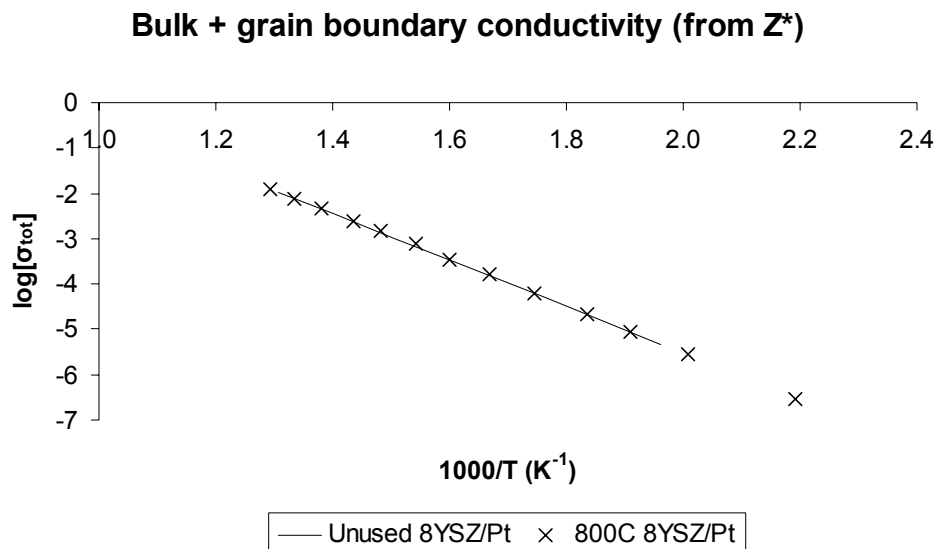
Bulk + grain boundary conductivity (from Z*)

Figure 13: Bulk and grain boundary conductivity against temperature for 8% yttria YSZ/Pt pellet before (line) and after (crosses) SO₂ exposure

A sub-test was performed to establish if the application of the potential across the pellet was responsible for the decreasing permeation performance. Between 2.0 and 2.5 hours into the run, SO$_2$ and O$_2$ were supplied to the membrane feed side whilst the electrical circuit was open. As shown in Figure 11 and Figure 12, no oxygen permeated

during this period and, following reapplication of the 1.00V potential, no recovery in membrane O_2 permeation performance was observed as a result of the open circuit period for either membrane. That the O_2 concentrations before and after the open circuit period describe a similar path suggests that the degradation in performance is independent of external voltage application or amount of O_2 permeating.

Another sub-test performed was to supply 10% O_2 only (i.e. no SO_2) to the pellets for one hour in order to determine if the pellet would recover some or all of the lost O_2 permeation performance. This was carried out between three and four hours into the run. Within five minutes of reapplying the SO_2-O_2-He feed, the permeate O_2 concentration decreases to that which, extrapolating the pre-recovery values, would be expected at that time. This suggests that replacing the SO_2-O_2-He feed with an O_2-He feed does not extend the membrane life but may merely mask a continuing decrease in performance. The surface effect which is suspected to be causing the performance decrease would appear to be non-reversible through a change in process conditions.

It can be seen from the ratios at the bottom of Table 1 that the YSZ/Au has a greater decrease in O_2 permeation over the course of the run compared to the YSZ/Pt pellet. Additionally, the YSZ/Au only "recovers" by 18% during the one hour O_2-He feed period, compared to the 88% O_2 permeation increase in the YSZ/Pt pellet. This shows that the decrease in O_2 permeation performance is electrode material dependent. The conductivity measurements shown in Figure 14 show that, like the YSZ/Pt pellet, the "bulk" of the pellet has been electrically unaffected by the SO_2 exposure and hence the performance decrease is likely to be related to the surface characteristics.

During both the YSZ/Au and YSZ/Pt pellet investigations at 800°C, fuming indicative of SO_3 production by catalysis at the metallic electrode was observed. The gold electrode therefore also acts catalytically on the SO_2 and O_2 being supplied.
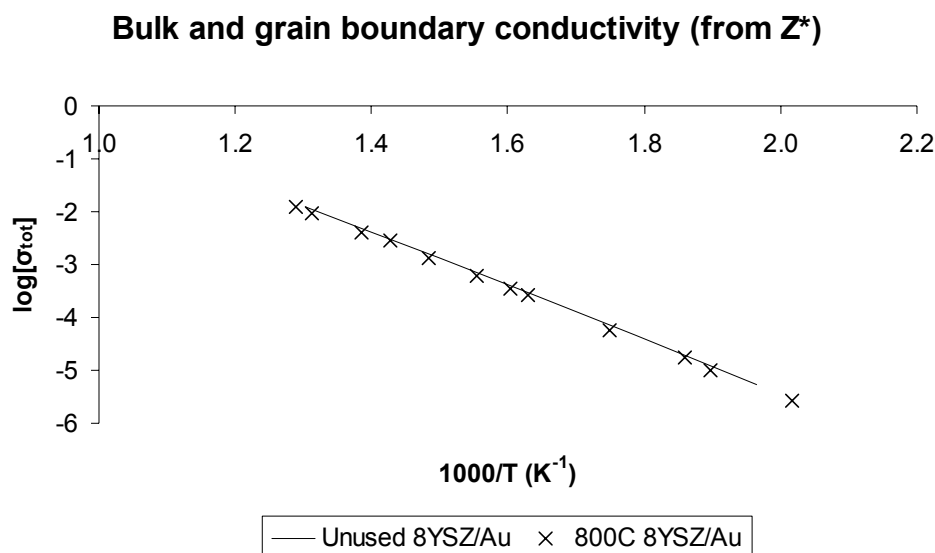

Figure 14: Bulk and grain boundary conductivity against temperature for 8% yttria YSZ/Au pellet before (line) and after (crosses) SO_2 exposure

Conclusions

Process simulations have shown that removing oxygen from the sulphuric acid thermal decomposition process can increase SO_2 yield at a given temperature and pressure. Yttria-stabilised zirconia (YSZ) is a potential dense membrane material for this process. Experiments have shown that whilst the bulk of a YSZ pellet is not affected by SO_2 exposure, a surface effect reduces the O_2 permeation flux at a given applied voltage. Investigations into the nature of this effect are ongoing.

References

[1]   Forsberg C, Trowbridge L, Bischoff B, Mansur LK. Sulfur thermochemical processes with inorganic membranes to produce hydrogen. AIChE Spring National Meeting, New Orleans, Louisiana, USA, 2004.

[2]   Ozturk IT, Hammache A, Bilgen E. An improved process for H2SO4 decomposition step of the sulfur-iodine cycle. Energy Convers Manage 1995;36(1):11-21.